コンクリート工学年次論文報告集 Vol. 17, No. 2 1995

論文 Flexural Behavior of RC L-Shaped Shear Walls under A Normal Force and BI-Directional Reversal Forces

Fouad KHAIRALLAH*, Yasuyuki ARAI*, Mitsuo MIZOGUCHI* and Chikara TAKEDA*

ABSTRACT: Six large scale identical L-shaped section walls were tested under the combined action of a constant axial force and bi-directional reversal horizontal forces increasing to failure. Strength and deformational characteristic revealed by the experimental results are very close to the values computed using the bi-directional bending strength method.
KEYWORDS: axial force, bi-directional strength, failure mechanism, flexural strength, L-shaped section, reinforced concrete, structural design, shear walls.

1. INTRODUCTION

The cost of seismic damage on the reinforced concrete structures and experiences drawn from earthquakes have strongly encouraged the use of vertical elements with large lateral stiffness. Designers may favor non-planar wall sections, such as L, T, U etc., to provide an efficient bracing system and to offer great potential for lateral load resistance. The responses of these types of walls with at least one cross-sectional axis but this is not a symmetry axis. Due to the unsymmetrical geometry, the walls will be governed by unsymmetric bending, and would be influenced by inelastic biaxial interaction.

An experimental program was designed to study 3-dimensional response of RC L-shaped walls under different loading histories. This paper describes the test results of six large scale identical L-shaped walls that were examined under the combined action of a constant axial force and bi-directional non-planar reversal horizontal forces. The horizontal forces were executed in different biaxial lateral paths to explain the flexural behavior of the examined walls. Also, the test results were compared with the values computed using the bi-directional bending strength method.

2. EXPERIMENTAL PROGRAM

2.1 TEST SPECIMENS

Six identical L-shaped walls were tested to failure. The nominal dimensions of the specimens, together with the arrangement of the displacement measuring scales, are shown in Figure 1. The walls were connected to upper and lower rigid slabs which are 300 mm thick. Double layer of 4-mm diameter mesh reinforcement wires with spacing of 60 mm was used in reinforcing the walls. The walls were enclosed by columns that were designed to fail in flexure and had the same thickness as the walls. Reinforcement bars of 10-mm diameter, and reinforcement wires of 4-mm diameter with spacing of 30 mm as spiral hoops

* Department of Civil Engineering and Architecture, Muroran Institute of Technology, Japan.

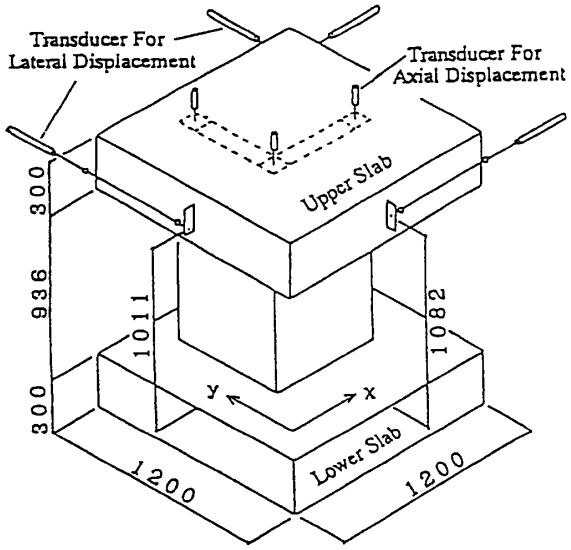

Figure 1 Details of Specimens (mm).

Table 1 Properties of Concrete Specimen.

Specimen	σ_B	$_c\sigma_t$	$E_{1/3}$
L-XN	311	29.0	2.47
L-UN	314	25.0	2.66
L-VN	319	25.0	2.66
L-UXN	319	30.8	2.65
L-CN	340	29.5	2.73
L-HN	308	26.0	2.65

σ_B : Compressive Strength(kg/cm²)
$_c\sigma_t$: Tensile Strength (kg/cm²)
$E_{1/3}$: Secant Modulus of Elasticity (× 10^5kg/cm²)

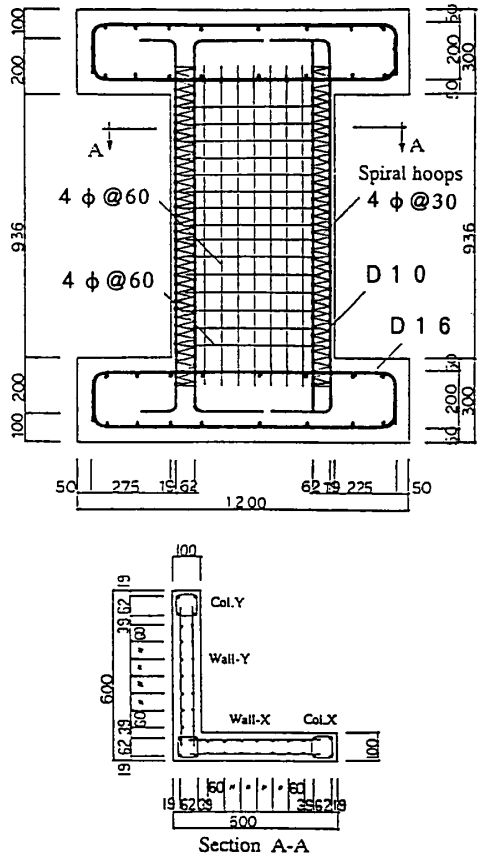

Figure 2 Details of Reinforcement.

Table 2 Properties of Reinforcement.

Reinforcement Type	Cross-Sectional Area (cm²)	Yielding Strength (kg/cm²)	Ultimate Strength (kg/cm²)	Elongation Percentage (%)
D10	(0.713)*	3820	5300	21.6
4 φ	0.122	2000	3140	38.6

( )* : Nominal Cross-Sectional Area.

were used in reinforcing the columns, full details of reinforcement are given in Figure 2. Normal concrete mixes with a maximum aggregate size of 10 mm were used for the specimens. Full details of material properties are given in Tables 1 and 2. The test specimens were named according to the lateral biaxial deflections acting at the top of the walls, as shown in Figure 3.

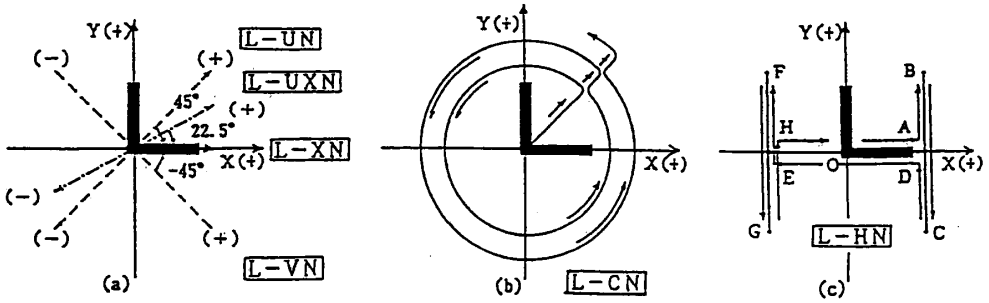

Figure 3 Specimens Names.

2.2 TESTING PROCEDURE

Each specimen was subjected to a combination of axial and horizontal loading using hydraulic actuators, as shown in Figure 4. Actuators (2) and (3) were adjusted to produce reversed gradual increments of the lateral deflections in X and Y-directions. Actuator (1) was adjusted to resist the horizontal torsion at the upper slab. The load applied by each actuator resolved into components in X and Y-directions. The resultant of the loads' component in X-direction was called X-load, and the same in Y-direction. The hydraulic jack was adapted to produce a constant axial force that corresponded to about 0.1 of the compressive strength of the wall section.

The reversed deflection increments were at rotation angles of 0.001, 0.002, 0.004, 0.006, 0.010, 0.015, 0.020 and 0.045 radians. Four linear variable transducers were used to monitor the lateral displacements and three to monitor the vertical displacements at the center of the columns, mounted as shown in Figure 1. Forty-four wire resistance strain gauges were employed to measure strains of the main reinforcing bars of columns and walls.

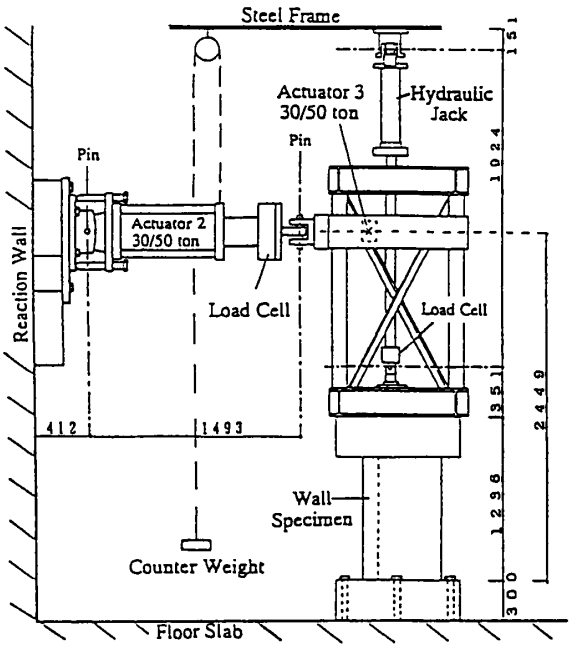

Figure 4 Loading Apparatus (mm).

3. TEST RESULTS

NOTE: Before discussing the experimental results, it is noteworthy that the base slab was made rigid enough and accordingly, the base rotations were negligible.

3.1 FRACTURE PROCESS

Flexural cracks initially appeared near the bottom of the walls. Gradually the inclined cracks appeared when the applied load reached about one third of the ultimate lateral load. Further loading caused new flexural and inclined cracks to develop and to reach the compressive zone, followed by starting of yield of the main reinforcing bars. At this stage, the

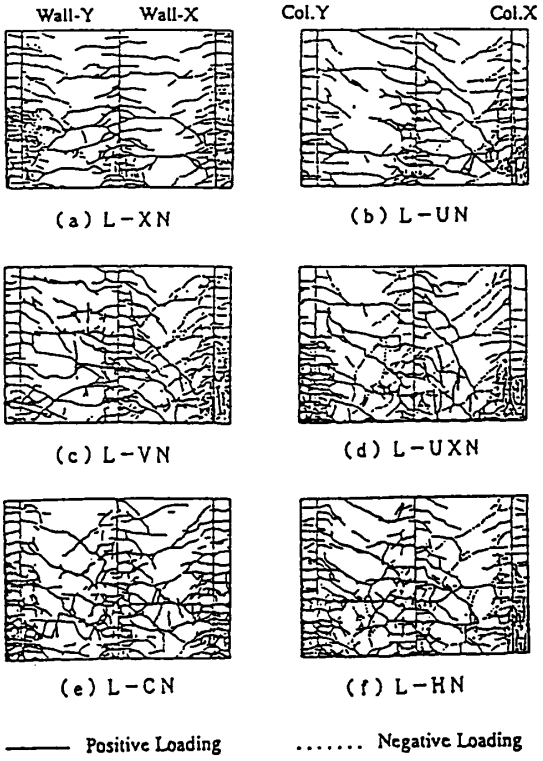

Figure 5 Cracking Patterns.

width of the major flexural cracks became considerable. Figure 5 gives the cracking patterns of the test specimens at failure.

3.2 LOAD-DEFLECTION RELATIONSHIP

The deformational response of the tested walls was found to be distinctly nonlinear in all cases, as shown in Figures 6 and 7. The significant difference between positive and negative responses for all the specimens except specimen L-VN may be attributed to the difference in the amounts of the effective tensile reinforcement. In case of specimen L-VN the effective tensile reinforcement was the same in both positive and negative directions. The load-carrying capacity of the specimens reduced gradually after the lateral horizontal load reached its ultimate value and this is attributed to the severe loosing of stiffness caused by spalling of concrete in the compressive zone.

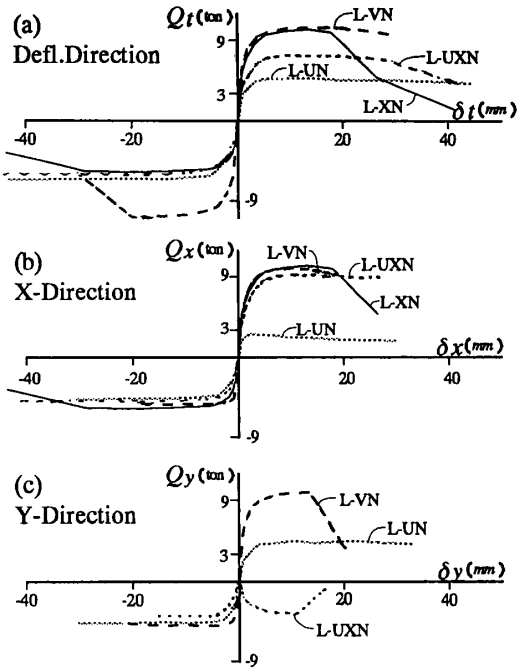

Figure 6 Max. Load-Deflection Curves at Each Cycle.

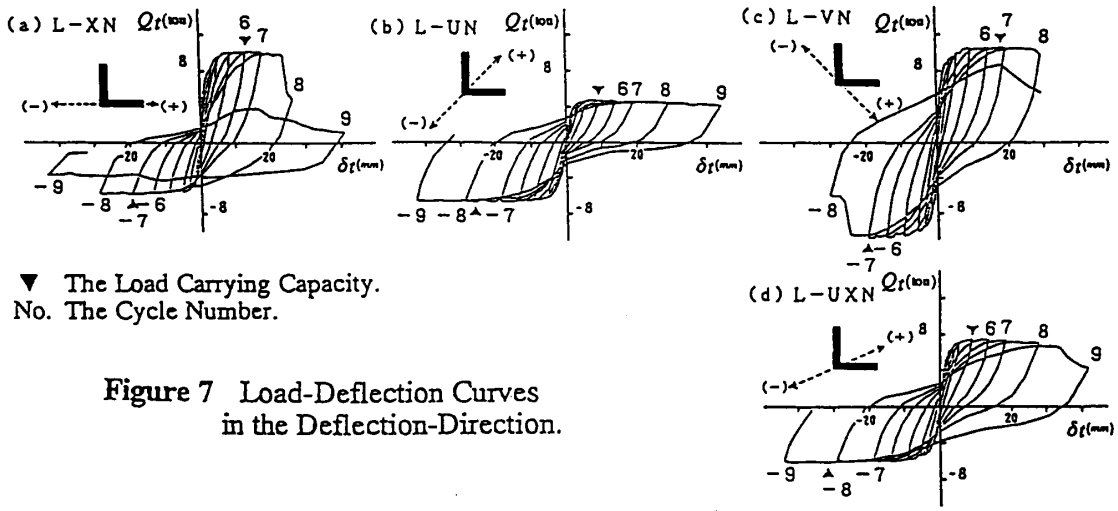

▼ The Load Carrying Capacity.
No. The Cycle Number.

Figure 7 Load-Deflection Curves in the Deflection-Direction.

3.3 ULTIMATE BENDING STRENGTH METHOD

The ultimate lateral load value ($_cQ_{BU}$) for the specimens is computed using the ultimate bending strength equation:

$$ {}_cQ_{BU} = \left\{ \sum_i \left(a_{s,i} \cdot \sigma_{sy,i} \cdot l_i \right) + N \cdot l_N \right\} / h $$

where

$(a_{s,i} \cdot \sigma_{sy,i})$ = Yield force of reinforcement group (i).
l_i, l_N = Horizontal displacements.
N = The effective axial force (33 tons).
h = The effective height of the lateral loads (2449 mm).

In Figure 8 the mark "+" is the center of the compressed column and the marks "O" is the center of the tensile reinforcement group. As detailed in Table 3, the ratios of the experimental result of the ultimate lateral load to the computed value ($_tQ_{BU}$ /$_cQ_{BU}$) varied from 0.94 in specimen L-UXN to 1.33 in specimen L-XN with an average of 1.06, indicating a good agreement. Figure 9 shows the results in polar coordinates.

3.4 BI-DIRECTIONAL BENDING STRENGTH DIAGRAM

The calculation method of the bi-directional bending strength diagram expressed on X-Y coordinates is given in Figure 10-(a). The triangle presented by the solid lines in Figure 11 is called bi-directional bending strength diagram. If one of the three columns is compressed (marked by "+") and the other two are tensioned (marked by "O"), there are three patterns of flexural failure presented by points [1], [3] and [5]. If any two columns are compressed equally, there are three patterns presented by points [2], [4] and [6], marked by "⊕".

The position of the compression center is necessary, because the forces Qx and Qy in the deflection direction may slightly spread out of the triangle after the third or the fourth cycle. As shown in Figure 10-(b), we can assume that the compression center slightly moves from the center of the compressed column to the reinforcing bars named (A) inside the same column, except in case of specimen L-UN in the positive direction. We assume that the compression center moves to the reinforcing bars named (B). According to this assumption the bi-directional bending strength triangle enlarged, and presented by the doted lines in Figure 11. The relationships between the lateral loads in X and Y-directions are shown in Figure 12, i.e., the maximum Qx and Qy in each cycle for specimens L-XN, L-UN, L-VN and L-UXN, but in each load increment for specimens L-CN and L-HN. The curves show a good accuracy in estimating the ultimate lateral loads of the L-shaped shear walls.

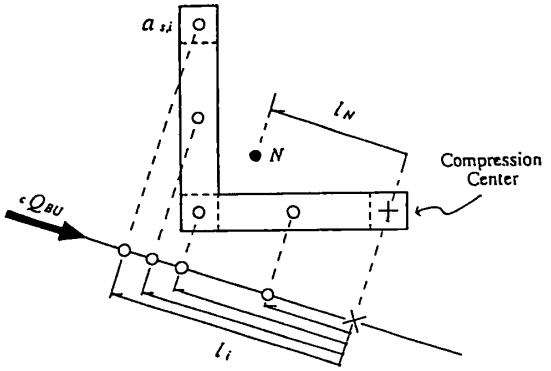

$$_cQ_{BU} = \left\{ \sum_i \left(a_{s,i} \cdot \sigma_{sy,i} \cdot l_i \right) + N \cdot l_N \right\} / h$$

Figure 8 Calculation Method for Bending Strength in Deflection Direction.

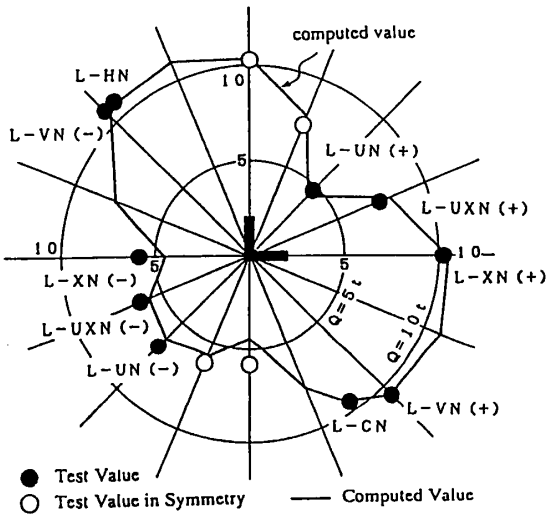

Figure 9 Bending Strength Diagram in Deflection Direction.

Table 3 Comparison of Theoretical and Experimental results.

Specimen	Direc-tion	Cycl No.	$_tQ_{BU}$(ton)	$_cQ_{BU}$(ton)	$\frac{_tQ_{BU}}{_cQ_{BU}}$
L-XN	+	6	10.31	10.40	0.99
	-	7	5.88	4.41	1.33
L-UN	+	5	4.81	4.23	1.14
	-	8	6.75	6.24	1.08
L-VN	+	7	10.61	10.47	1.01
	-	7	10.80	10.47	1.03
L-UXN	+	5	7.42	7.91	0.94
	-	9	6.20	5.77	1.07
L-CN	304°	6	9.45	9.5	0.99
L-HN	131°	5	10.83	10.74	1.01

$_tQ_{BU}$: Experimental Ultimate Lateral Load.
$_cQ_{BU}$: Computed Value.

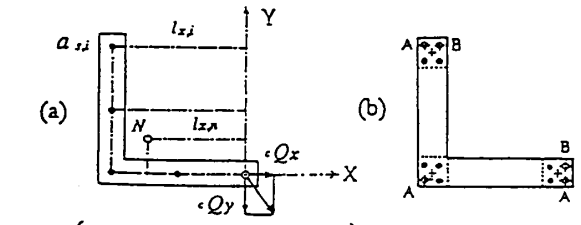

$$\circ Qx = \left\{ \sum_i \left(a_{s,i} \cdot \sigma_{sy,i} \cdot l_{x,i} \right) + N \cdot l_{x,n} \right\} / h$$

$$\circ Qy = \left\{ \sum_i \left(a_{s,i} \cdot \sigma_{sy,i} \cdot l_{y,i} \right) + N \cdot l_{y,n} \right\} / h$$

Figure 10 Calculation Method for Bi-Directional Bending Strength.

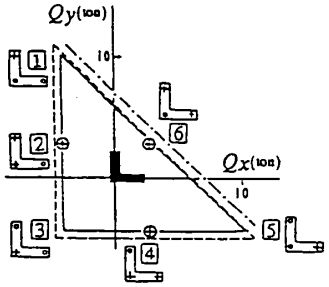

Figure 11 Bi-Directional Bending Strength Diagram.

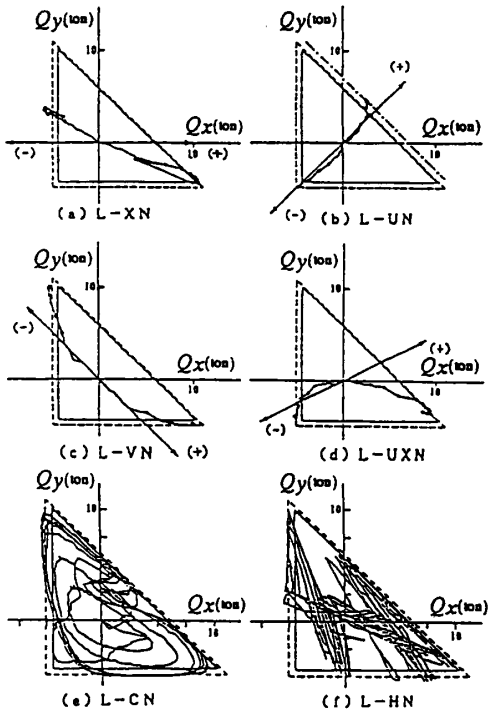

Figure 12 The Lateral Loads Q x and Q y.

4. CONCLUSIONS

This paper presents an experimental study on non-planar L-shaped shear walls under the combined action of a constant axial force and bi-directional reversal horizontal forces. The following conclusions can be revealed:

1. The bi-directional bending strength method represents a reliable and accurate method for calculating the ultimate lateral loads of non-planar L-shaped shear walls subjected to a constant axial force and bi-directional reversal horizontal forces.
2. The load-carrying capacity of non-planar L-shaped shear walls subjected to lateral displacement along different biaxial paths depends mainly on the effective tensile flexural reinforcement.

REFERENCES

1. Huria, V., Raghavendrachar, M. and Aktan, A. E. "3-D Characteristics of RC Wall Response." Journal of Struct. Engng, ASCE, Vol. 117, No. 10, Oct., 1991, pp. 3149-3167.
2. Lefas, I., Kotsovos, M. and Ambraseys, N. "Behavior of Reinforced Concrete Structural Walls: Strength, Deformation Characteristics, and Failure Mechanism." ACI Structural Journal, Vol. 87, No. 1, Jan., 1990, pp. 23-31.
3. Mizoguchi, M. and Arai, Y. "Elasto-Plastic Properties of Reinforced Concrete L-shaped Section Shear Walls Subject to Bi-directional Horizontal Force." Journal of Struct. Constr. Engng, AIJ, No. 450, Aug., 1993, pp. 71-80.(in Japanese).
4. Mizoguchi, M. and Arai, Y. "Elasto-Plastic Properties of Reinforced Concrete L-shaped Section Shear Walls Subject to Bi-directional Horizontal Force (Part 2). Bi-directional bending ultimate strength." Journal of Struct. Constr. Engng, AIJ, No. 464, Oct., 1994, pp. 101-108.(in Japanese).